



## Metabolic and physiological alterations indicate that the tropical broadleaf tree *Eugenia uniflora* L. is sensitive to ozone

Marcela Regina Gonçalves da Silva Engela<sup>a,\*</sup>, Claudia Maria Furlan<sup>b</sup>, Marisia Pannia Esposito<sup>b</sup>, Francine Faia Fernandes<sup>a</sup>, Elisa Carrari<sup>c</sup>, Marisa Domingos<sup>a</sup>, Elena Paoletti<sup>c</sup>, Yasutomo Hoshika<sup>c</sup>

<sup>a</sup> Institute of Botany, Ecology Research Center, Avenue Miguel Estéfano, 3687, 04301-012, SP, Brazil

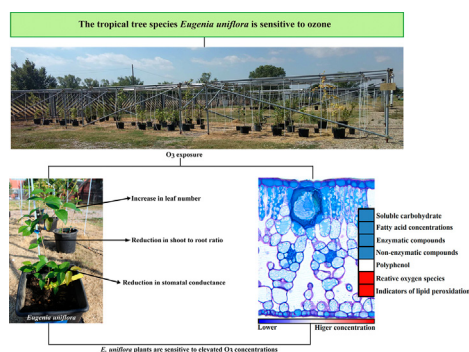
<sup>b</sup> Institute of Bioscience, University of São Paulo, Matão St. 257, 05508-090, SP, Brazil

<sup>c</sup> Institute of Research on Terrestrial Ecosystems (IRET), National Research Council (CNR), Via Madonna del Piano 10, 50019 Sesto Fiorentino, Italy

### HIGHLIGHTS

- *Eugenia uniflora* plants were exposed to realistic ozone pollution in a O<sub>3</sub>-FACE system.
- An inefficient antioxidant response was observed under elevated O<sub>3</sub> level.
- Metabolic and physiological alterations were markers of oxidative damage.
- Enhanced contents of sugar alcohols may minimize the O<sub>3</sub> effects.
- *E. uniflora* is to be considered an O<sub>3</sub> sensitive species.

### GRAPHICAL ABSTRACT



### ARTICLE INFO

#### Article history:

Received 16 September 2020

Received in revised form 18 December 2020

Accepted 7 January 2021

Available online 15 January 2021

Editor: Charlotte Poschenrieder

#### Keywords:

Carbohydrates

Flavonoids

Reactive oxygen species

Photosynthesis

Growth and biomass

Tropical species

### ABSTRACT

*Eugenia uniflora* L. is an important fruit tree native to tropical South America that adapts to different habitats, thanks to its metabolic diversity and ability to adjust the leaf antioxidant metabolism. We hypothesized that this metabolic diversity would also enable *E. uniflora* to avoid oxidative damage and tolerate the enhanced ozone (O<sub>3</sub>) concentrations that have been registered in the (sub)tropics. We investigated whether carbohydrates, polyphenols and antioxidants are altered and markers of oxidative damage (ROS accumulation, alterations in leaf gas exchange, growth and biomass production) are detected in plants exposed to two levels of O<sub>3</sub> (ambient air and twice elevated ozone level in a O<sub>3</sub>-FACE system for 75 days). Phytotoxic O<sub>3</sub> dose above a threshold of 0 nmol m<sup>-2</sup> s<sup>-1</sup> (POD0) and accumulated exposure above 40 ppb (AOT40) were 3.6 mmol m<sup>-2</sup> and 14.898 ppb h at ambient, and 4.7 mmol m<sup>-2</sup> and 43.881 ppb h at elevated O<sub>3</sub>. Twenty-seven primary metabolites and 16 phenolic compounds were detected in the leaves. Contrary to the proposed hypothesis that tropical broadleaf trees are relatively O<sub>3</sub> tolerant, we concluded that *E. uniflora* plants are sensitive to elevated O<sub>3</sub> concentrations. Experimental POD0 values were lower than the critical levels for visible foliar O<sub>3</sub>, because of low stomatal conductance. In spite of this low stomatal O<sub>3</sub> uptake, we found classic O<sub>3</sub> injury, e.g. reduction in carbohydrates and fatty acids concentrations; non-significant changes in the polyphenol profile; inefficient antioxidant responses; increased contents of ROS and indicators of lipid peroxidation; reductions in stomatal conductance, net photosynthesis, root/shoot ratio and height growth. However, we also found some compensation mechanisms, e.g. increased leaf concentration of polyols for protecting the membranes, and increased leaf number for compensating the decline of photosynthetic rate. These results help filling the knowledge gap about tropical tree responses to O<sub>3</sub>.

© 2021 Elsevier B.V. All rights reserved.

\* Corresponding author.

E-mail address: [marcelaengela@gmail.com](mailto:marcelaengela@gmail.com) (M.R.G.S. Engela).

## 1. Introduction

*Eugenia uniflora* L. is an important broadleaf fruit tree native to tropical South America (Auricchio and Bacchi, 2003; Melo et al., 2007; Denardin et al., 2015). However, this species is widespread in several tropical and subtropical areas, from Asia to the Caribbean (Garmus et al., 2014) due to its high plasticity and capacity to grow in different soil and climate conditions.

Several studies indicate that *E. uniflora* polyphenol composition is effective against some bacteria, has diuretic, anti-rheumatic, antifebrile and anti-inflammatory actions and therapeutic potential for stomach diseases (Da Cunha et al., 2016; Sobeh et al., 2019). Furthermore, *E. uniflora* leaf extracts show high antioxidant potential related to polyphenol composition, especially flavonoids and tannin contents (Kade et al., 2008; Mesquita et al., 2017; Souza et al., 2018).

*E. uniflora* has potentially been exposed to increasing ozone ( $O_3$ ) pollution throughout its occurrence area. This pollutant is the most damaging phytotoxic air pollutant because of its oxidative potential (Paoletti et al., 2017; Bloss, 2018). It has caused adverse effects on forest health and biodiversity all around the world, including the tropics and subtropics (Gerken et al., 2016; Pope et al., 2019; Paralovo et al., 2019; Li et al., 2020; Siciliano et al., 2020).

The  $O_3$  toxicity level to plants will depend on their capacity of maintaining cellular homeostasis, by mobilizing antioxidants, such as enzymes (e.g. ascorbate peroxidase, catalase, glutathione reductase and superoxide dismutase) and non-enzymatic compounds (e.g., ascorbic acid and glutathione) of the ascorbate-glutathione cycle (Aguiar-Silva et al., 2016; Brandão et al., 2017). Plants may also adjust their primary and secondary metabolisms, thus increasing their tolerance against oxidative stress (Domingos et al., 2015). Soluble carbohydrates (e.g., fructose, glucose and sucrose) are regulatory molecules that control gene expression related to metabolism, stress resistance, growth and development. Sugar alcohols (e.g., *myo*-inositol) exert an important role in scavenging hydroxyl radicals originated from lipid peroxidation (Peshev & Van den Ende, 2013; Du et al., 2018; Shu et al., 2019). Polyphenols, such as flavonoids (e.g. flavonols) and tannins, besides repelling herbivores and attracting pollinators (War et al., 2012; Tuominen, 2013; Mouradov and Spangenberg, 2014) may also scavenge free radicals (Booker et al., 2012; Richet et al., 2012; Mierziak et al., 2014).

Although  $O_3$  is an important environmental issue in tropical and subtropical areas (Dong et al., 2020; Takahashi et al., 2020), there is few knowledge available on the  $O_3$  impacts in native plant species at these areas. For example, it is known that gas exchange of subtropical broadleaf species was less impaired by  $O_3$  than that of broadleaf species from temperate climates (Li et al., 2017); however, the effective  $O_3$  flux into subtropical plants has rarely been estimated (Agathokleous et al., 2020; Cardoso-Gustavson et al., 2020).

In this study, we assumed that the capacity of *E. uniflora* to occupy different habitats is derived from the ability to alter its metabolic profile. We hypothesized that such leaf traits would also enable the species to avoid oxidative damage and tolerate elevated  $O_3$  concentrations. We investigated whether the composition and concentrations of carbohydrates and polyphenols, and levels of antioxidants are altered and whether markers of oxidative damage (ROS accumulation and alterations in leaf gas exchange, growth and biomass production) are detected in plants of *E. uniflora* growing under elevated  $O_3$  levels in an  $O_3$ -Free-Air Controlled Exposure ( $O_3$ -FACE) system.

## 2. Materials and methods

### 2.1. Experimental design

Seedlings of *E. uniflora* (6-month-old and approx. 20 cm high) were obtained from a Brazilian nursery (23°22'18" S, 45°39'52" W) and sent to Italy in May 2017. The seedlings were then transplanted to 1.7 L

pots filled with a mixture of sand: peat: nursery soil (1:1:1, v/v). Plants were irrigated every day by a drip system to avoid water stress (i.e., volumetric soil water content was maintained to the field capacity of  $\approx 0.295 \text{ m}^3 \text{ m}^{-3}$ ). The experiment was carried out in an  $O_3$ -FACE system located in Sesto Fiorentino, Florence, Italy (43°48'59" N, 11°12'01" E, 55 m a.s.l.). Details of the exposure facility are given in Paoletti et al. (2017). The plants were submitted to two  $O_3$  levels: ambient air and elevated  $O_3$  during 75 days of summer season (from July 10th to September 25th 2017). The system consisted of three plots per  $O_3$  treatment; each plot was considered as a replicate ( $n = 3$ ). Six pots of *E. uniflora* were maintained in each plot (totaling 18 plants per  $O_3$  treatment = 36 plants).

The  $O_3$  concentration was continuously monitored by active  $O_3$  monitors (Mod. 202, 2B Technologies, Boulder CO, USA). Global solar radiation (GSR), air temperature (Temp), relative humidity (RH) and precipitation (P) were continuously recorded by a Watchdog station (Mod. 2000; Spectrum Technology, Inc., Aurora, IL, USA) at 2.5 m a.g.l.

### 2.2. Metabolite profile

Metabolite profiles were analyzed at the end of the experiment in composite leaf samples of three fully expanded and sun-exposed leaves per plant from each plot, totaling 18 composite leaf samples per  $O_3$  treatment. The samples were stored in an ultra-freezer, at  $-80^\circ\text{C}$ , until analyses.

#### 2.2.1. Compounds detected by GC-EIMS

Leaf material (20 mg) was extracted in 500  $\mu\text{L}$  of methanol/chloroform/water (12:5:1, v/v) and 50  $\mu\text{L}$  of ribitol (0.2 mg  $\text{mL}^{-1}$ ) added as internal standard, according to a modified version of the method described by Suguiyama et al. (2014). Samples were analyzed using gas chromatography coupled to mass spectrometry (GC-EIMS 6850/5975B Agilent Technologies) with a capillary column VF-5MS column (Agilent, length 30 m, ID 250  $\mu\text{m}$ , 0.25  $\mu\text{m}$  film thickness) and a pre-column (0.25 mm  $\times$  10 m). The injection volume was 1  $\mu\text{L}$  using Helium as mobile phase (1.0  $\text{mL min}^{-1}$ ). Temperature was programmed as isothermal for 5 min at  $70^\circ\text{C}$ , followed by a  $5^\circ\text{C per min}$  ramp to  $295^\circ\text{C}$ . The injector, ion source, and quadrupole temperatures were  $230^\circ\text{C}$ ,  $200^\circ\text{C}$ , and  $150^\circ\text{C}$ , respectively. The EIMS analysis employed an ionization voltage of 70 eV; the recorded mass range was of  $m/z$  50 to  $m/z$  600 at 2 scan/s. Substances were identified and compared with authentic standards and using NIST (National Institute of Standards and Technology) digital library spectra (v2.0, 2008) and GNPS (Global Natural Products Social Molecular Networking) spectral library (2016). The Linear Index of Retention was calculated for each compound using the alkane standard according to Viegas and Bassoli (2007).

#### 2.2.2. Phenolic compounds detected by HPLC-DAD-MS

Phenolic compounds were extracted from the freeze-dried leaves (100 mg) using 5 mL of 80% methanol (MeOH), and the final volume of the extract was adjusted to 10 mL. The extract was filtered (0.45  $\mu\text{m}$ ) and analyzed by High Performance Liquid Chromatography coupled to a diode array detector (HPLC-DAD), Agilent 1260 Analytic with Zorbax Eclipse Plus C18 column (4.6  $\times$  150 mm, 3.5  $\mu\text{m}$ ) at  $45^\circ\text{C}$ . The mobile phase had a constant flow of 1  $\text{mL min}^{-1}$  and a gradient elution of 0.1% acetic acid (A) and acetonitrile (B), starting with 90% (A) for 6 min, decreasing to 85% (A) for the next 1 min and maintaining for 15 min, decreasing to 50% (A) for 10 min, and decreasing to 0% (A) for the next 10 min, maintaining isocratic for the last 8 min (total run time 50 min). A post-run of 5 min was applied to return to the initial conditions. Phenolic compounds were detected at 280 and 352 nm. Contents of each compound were estimated using quercetin (1.5 to 150  $\mu\text{g/mL}$ ;  $y = 17,023x - 4.5312$  and  $R^2 = 0.9998$ ).

For the identification, the samples were submitted to high performance liquid chromatography coupled to mass spectrometry (HPLC-

MS/MS). The equipment used was the HPLC-30AD Shimadzu coupled to the SPD-20A and Amazon Speed ETD Bruker detectors, using the Zorbax Eclipse Plus C18 (150 × 4.6 nm, 3.5 mm - Agilent) column. For mass spectrometry the conditions were: ESI 500 V source, 4500 V capillary voltage, 27 Psi nebulizer, 325 °C drying gas and 12 L min<sup>-1</sup> flow. The acquisition took place in negative and positive module.

### 2.3. Antioxidant compounds from ascorbate-glutathione cycle

Non-enzymatic and enzymatic antioxidants were also measured on the composite samples stored at -80 °C. Three analytical replicates were performed per leaf sample.

Ascorbic acid was analyzed using the chromatographic method described by López et al. (2005) and a HPLC (Metrohm) connected to an UV-Vis detector. Portions of leaves (250 mg) were homogenized with 6% metaphosphoric acid and 0.5 mM EDTA-Na2. The supernatant was filtered through a paper filter (Whatman no. 41), and the filtrate was diluted with water. Glutathione content was spectrophotometrically determined according to the method described by Israr et al. (2006), where leaves (1.0 g) were homogenized with 0.1% sulfosalicylic acid. A mixture of 100 mM phosphate buffer (pH 7.0), 0.5 mM ethylenediaminetetraacetic acid - EDTA, and 3 mM 5.5'-dithio-bis-(1-nitrobenzoic acid) - DTNB was added to an aliquot of the supernatant. Ascorbate peroxidase (APX), catalase (CAT), glutathione reductase (GR) and superoxide dismutase (SOD) were analyzed by UV-vis spectrophotometry and their activities were analyzed in extracts of leaves prepared with 50 mM potassium phosphate buffer (pH 7.0), 0.05% triton, 10% polyvinyl pyrrolidone - PVPP, and 1 mM ascorbic acid. APX and SOD activities were determined according to Reddy et al. (2004). The APX activity was determined at 30 °C in a reaction mixture with 100 mM potassium phosphate buffer (pH 7.0), 1 mM EDTA, 5 mM ascorbic acid, and 2 mM hydrogen peroxide, measured at 290 nm. The SOD activity was determined by measuring the ability of the enzyme to inhibit the photochemical reduction of nitroblue tetrazolium (NBT) at 560 nm. CAT activity was determined as described by Kraus et al. (1995) with some modifications proposed by Azevedo et al. (1998). At 25 °C, the supernatant was added to a reaction mixture of 1 mL of 100 mM potassium phosphate buffer (pH 7.5) and 1 mM hydrogen peroxide that was prepared immediately before use. The activity was set by monitoring the removal of H<sub>2</sub>O<sub>2</sub> at 240 nm over 1 min. The activity of glutathione reductase (GR) was determined according to the method of Reddy et al. (2004) in leaves (1.0 g) that had been homogenized with 50 mM potassium phosphate buffer (pH 7.8), 5 mM ascorbic acid, 5 mM EDTA, and 5 mM 1.4 dithiothreitol - DTT, measured at 412 nm. Further analytical details about enzymatic and non-enzymatic compounds can be found in Esposito et al. (2016).

### 2.4. Markers of oxidative damage

The following markers of oxidative damage were measured on the composite samples stored at -80 °C. Three analytical replicates were performed per leaf sample and their average was used in the statistical analyses, as the statistical unit was the individual plot ( $n = 3$  plots).

#### 2.4.1. Indicators of lipid peroxidation (malondialdehyde and hydroperoxide conjugated diene)

The concentrations of malondialdehyde (MDA) were determined following the method proposed by Hodges et al. (1999) with the corrected equation proposed by Landi (2017), where the plant material was homogenized in 0.1% trichloroacetic acid containing PVPP. Trichloroacetic acid containing thiobarbituric acid was added to the supernatant, which was maintained for 30 min at 95 °C in a water bath. The concentrations of hydroperoxide conjugated diene (HPCD) were obtained from leaves in ethanol (96%) by spectrophotometric UV-Vis method after a dilution of 1:15 (Levin and Pignata, 1995).

#### 2.4.2. Reactive oxygen species

The principle of the •OH radical assay was the quantification of the 2-deoxyribose degradation product MDA, by its condensation with thiobarbituric acid (TBA) (Lopes et al., 1999). The reaction mixture to determinate the H<sub>2</sub>O<sub>2</sub> contents consisted of supernatant extract (leaves + trichloroacetic acid), potassium phosphate buffer (100 mM, pH 7.0) and reagent potassium iodide (KI) (Alexieva et al., 2001). The O<sub>2</sub>•<sup>-</sup> production rate was determined using the hydroxylamine oxidation method (Wang and Luo, 1990) with some modifications. Further analytical details about ROS and indicators of oxidative stress can be found in Esposito et al. (2018).

#### 2.4.3. Leaf gas exchange in light-saturated conditions

Gas exchange measurements of fully expanded sun leaves (3th to 5th from the shoot tip, 1 leaf per 1 to 3 plants per replicated plot,  $n = 3$  plots per each O<sub>3</sub> treatment) were carried out on 27 July and 6-7 September 2017 by a portable infrared gas analyzer (CIRAS-2 PP Systems, Herts, UK) at photosynthetic photon flux density (PPFD) of 1500 μmol m<sup>-2</sup> s<sup>-1</sup>, ambient CO<sub>2</sub> concentration of 400 μmol mol<sup>-1</sup>, relative humidity of 40 to 60% and leaf temperature of 25 °C, from 9:00 to 12:00 h. We determined the light-saturated net photosynthetic rate ( $A_{sat}$ ) and stomatal conductance for water vapor ( $g_{sw}$ ).

#### 2.4.4. Growth and biomass

At the end of the exposure period, plant growth was assessed on all plants by measuring plant height, stem diameter (near the base) and total number of leaves. For measurements of height and stem diameter, a measuring tape and a digital caliper (data expressed in cm) (Digimess, São Paulo, Brazil) were used (Sá et al., 2014), respectively.

Leaves, stems/branches and roots of each plant were then harvested, dried in an oven at 60 °C and weighted in order to estimate their biomass on a dry weight basis. Shoot to root ratios were then calculated according to Moura et al. (2018).

### 2.5. Calculation of phytotoxic ozone dose (POD)

The phytotoxic ozone dose (POD), i.e. the stomatal uptake above an hourly threshold of 0 nmol m<sup>-2</sup> s<sup>-1</sup> along the experiment (POD<sub>0</sub>), was determined as:

$$POD_0 = \sum_{i=1}^n (F_{st,i}) \cdot \Delta t, \quad (1)$$

where  $\Delta t = 1$  h is the averaging period,  $F_{st,i}$  is the  $i$ th hourly stomatal O<sub>3</sub> uptake (nmol m<sup>-2</sup> s<sup>-1</sup>), and  $n$  is the number of hours included in the calculation period. To estimate  $F_{st,i}$ , we applied the methodology recommended by the Mapping Manual of the Convention on Long-Range Transboundary Air Pollution for species-specific stomatal responses (CLRTAP, 2017). Stomatal conductance for O<sub>3</sub> ( $g_{sO_3}$ ) was estimated by a multiplicative stomatal conductance model (CLRTAP, 2017):

$$g_{sO_3} = g_{max} \cdot f_{light} \cdot f_{O_3} \cdot \max \left\{ f_{min}, \left( f_{temp} \cdot f_{VPD} \right) \right\}, \quad (2)$$

where  $g_{max}$  is the maximum stomatal conductance (mmol O<sub>3</sub> m<sup>-2</sup> Projected Leaf Area [PLA] s<sup>-1</sup>),  $f_{min}$  is the minimum stomatal conductance,  $f_{light}$ ,  $f_{O_3}$ ,  $f_{temp}$  and  $f_{VPD}$  account for stomatal responses to photosynthetic photon flux density (PPFD), O<sub>3</sub> concentration, air temperature (T) and vapor pressure deficit (VPD), respectively. It is known that high O<sub>3</sub> concentrations may reduce  $g_{sO_3}$  (Hoshika et al., 2020c). We therefore applied a simple linear function to explain the variation of  $g_{sO_3}$  with O<sub>3</sub> concentration as reported in rice leaves (Oue et al., 2008). It is given by:

$$f_{O_3} = 1 - b \cdot [O_3], \quad (3)$$

where  $b$  is a slope of the linear regression of  $f_{O_3}$  and  $[O_3]$  is an hourly O<sub>3</sub> concentration (ppb). For details of the other functions ( $f_{light}$ ,  $f_{temp}$  and

$f_{VPD}$ ) see CLRTAP (2017). The function describing modification of  $g_{sO_3}$  by soil moisture (i.e.,  $f_{SW}$ ) was not used in this study because soil moisture was kept to the field capacity throughout the experiment.

Parameterization was carried out using a boundary line analysis (Alonso et al., 2008; Braun et al., 2010; Hoshika et al., 2012, 2020). In addition to the measurements under light-saturated conditions, the daily profile (morning: 9:00 h, midday: 12:00 h, afternoon: 15:00 h) of stomatal conductance was measured on 18 July, 30 August and 8 September 2017. Diurnal course measurements were made under natural conditions of T, relative humidity and PPFD by a portable infra-red gas analyzer (CIRAS-2, PP Systems, Herts, UK) in order to take measurements with a various range of environmental factors (Hoshika et al., 2012). Pooled data (119 data points) were used to estimate the parameters. The stomatal conductance data were divided into classes with the step-wise increases for each variable as follows: 200  $\mu\text{mol photons m}^{-2} \text{s}^{-1}$  for PPFD (when PPFD < 200  $\mu\text{mol photons m}^{-2} \text{s}^{-1}$ , PPFD classes with 50  $\mu\text{mol photons m}^{-2} \text{s}^{-1}$  steps were adopted), 20 ppb for  $\text{O}_3$  concentration, 2 °C for T and 0.2 kPa for VPD. Model functions were fitted against each variable based on 95th percentile values per each class of environmental factors. Values of  $g_{\text{max}}$  and  $f_{\text{min}}$  were calculated as the 95th percentile and 5th percentile, respectively (Hoshika et al., 2012; Bičárová et al., 2019).

## 2.6. Data analysis

Significant differences between treatments for all parameters were determined by Student's *t*-test using Sigma Plot 11.0. To assess the

effects of  $\text{O}_3$  and measuring month on leaf gas exchange, a two-way analysis of variance (ANOVA) was applied. If necessary, an appropriate transformation of the data was performed to reach normal distribution and equal variances. Results were considered significant at  $p < 0.05$ .

The metabolite concentrations were also log2 transformed and analyzed via the *Heatmap* tool using the *Morpheus* platform, in order to determine the ratio between the metabolites identified in leaf samples from ambient air and elevated  $\text{O}_3$ .

## 3. Results

### 3.1. Environmental conditions during the experimental period

During the experimental period, the mean daily values of air temperature, global solar radiation, relative humidity and total daily precipitation varied between 19 and 32 °C, 57 and 434  $\text{W/m}^{-2}$ , 29 and 86%, and 0 and 62 mm, respectively (Fig. 1A). The mean daily  $\text{O}_3$  concentrations varied between 17 and 89 ppb at ambient air and 23–118 ppb at elevated  $\text{O}_3$  (Fig. 1B). After 75 days, the accumulated exposure over an hourly threshold of 40 ppb (AOT40) reached 14,898 ppb h at ambient air and 43,881 ppb h at elevated  $\text{O}_3$ .

### 3.2. Metabolite profile

#### 3.2.1. Compounds detected by GC-EIMS

GC-EIMS analyses of *E. uniflora* leaves revealed 27 major metabolites as follow: 13 carbohydrates (6 soluble sugars and 7 sugar

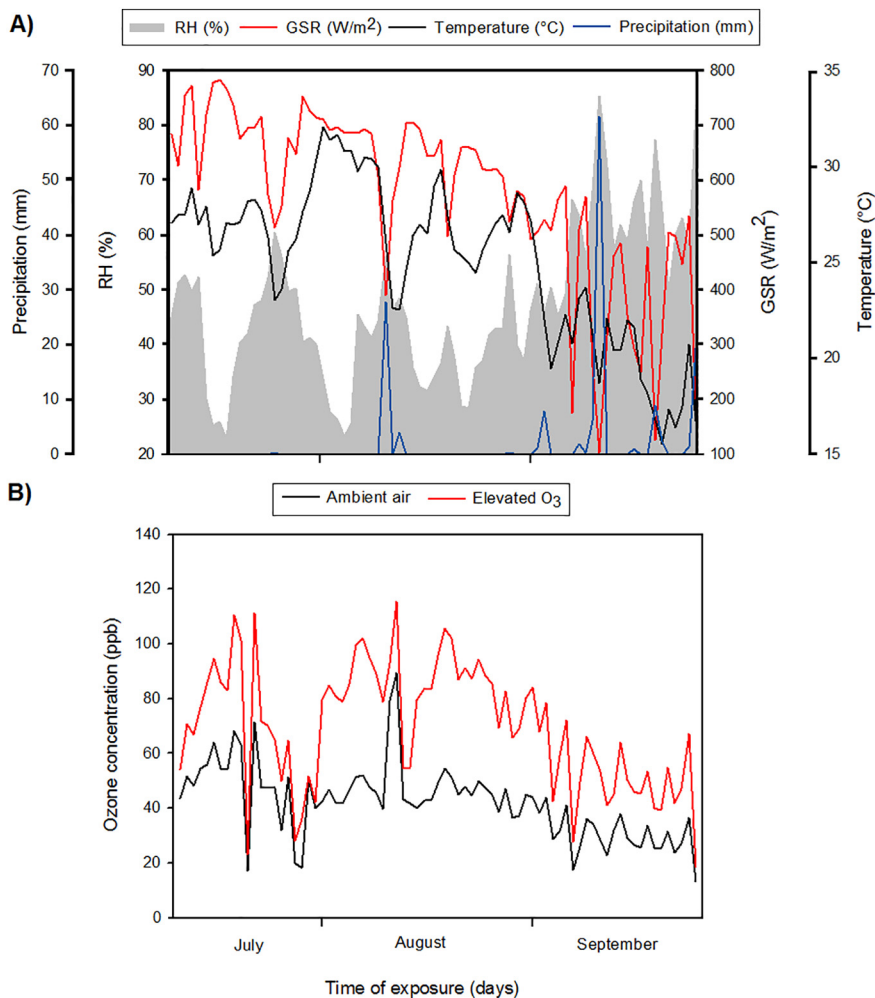


**Fig. 1.** Environmental conditions over the experimental period (from July 10th to September 25th 2017 = 75 days of exposure). (A) Daily mean values of temperature, relative humidity (RH %), global solar radiation (GSR), total daily precipitation and (B) ozone concentrations (ppb) at ambient air and at elevated  $\text{O}_3$  treatments.



alcohols), 6 fatty acids, 2 organic acids, ascorbic acid, 2 amino acids, 2 phenolic compounds, and 1 alkane (Table S1 and Fig. S1; supplementary material). Plants exposed to elevated O<sub>3</sub> presented significantly lower concentrations of all soluble sugars, amino acids (−26% threonine and −30% serine) and fatty acids (−38% tetradecanoic acid, −45% heptadecanoic acid, −19% octadecanoic acid and −26% stearic acid), but higher contents of all sugar alcohols than plants exposed to ambient air (Fig. 2A).

The heatmap analysis showed that the most evident differences between the treatments were observed for sucrose, glucopyranose, *myo*-inositol, ascorbic acid, heptadecanoic acid and tetradecanoic acid (Fig. 2B).

### 3.2.2. Phenolic compounds detected by HPLC-DAD-MS

Sixteen phenolic compounds were identified in *E. uniflora* leaves, being 14 flavonols (quercetin and myricetin derivatives), 2 cinnamic acid derivatives as caffeic acid glucoside and chlorogenic acid (Table S2 and Fig. S2; supplementary material). The foliar content of phenolic compounds did not differ significantly between treatments (Fig. 3A and B).

### 3.2.3. Antioxidant compounds from ascorbate-glutathione cycle

The leaf content of the reduced form of non-enzymatic compounds – ascorbic acid (AsA) and glutathione (GSH) – and the activity of enzymes

APX, CAT, GR, and SOD were significantly decreased in plants grown in the elevated O<sub>3</sub> when compared to ambient air (Fig. 4).

### 3.3. Markers of oxidative damage

The contents of MDA, HPDC, OH, H<sub>2</sub>O<sub>2</sub> and O<sub>2</sub><sup>−</sup> increased significantly 34%, 30%, 18%, 14% and 41%, respectively, in plants exposed to elevated O<sub>3</sub> when compared to plants exposed to ambient air (Fig. 5).

Light-saturated net photosynthetic rate (*A*<sub>sat</sub>) differed significantly between O<sub>3</sub> treatments (Fig. 6), with a decrease of 41% in July, and 31% in September. In addition, *g*<sub>sw</sub> decreased by 41% and 34% on average in July and September, respectively, in plants exposed to elevated O<sub>3</sub> compared to plants exposed to ambient air.

The leaf biomass significantly increased by 55% in plants exposed to elevated O<sub>3</sub> when compared to plants exposed to ambient air (Table 1). The biomass of stems and roots did not vary significantly between the O<sub>3</sub> treatments. However, the root to shoot ratio was decreased by 23% in the plants exposed to elevated O<sub>3</sub> relative to the ambient air plants. The height significantly decreased by 10% in the plants exposed to elevated O<sub>3</sub> when compared to the ambient air. The stem diameter did not vary significantly between the O<sub>3</sub> treatments. However, the number of leaves was 21% higher in the plants exposed to elevated O<sub>3</sub> than in the ambient air.

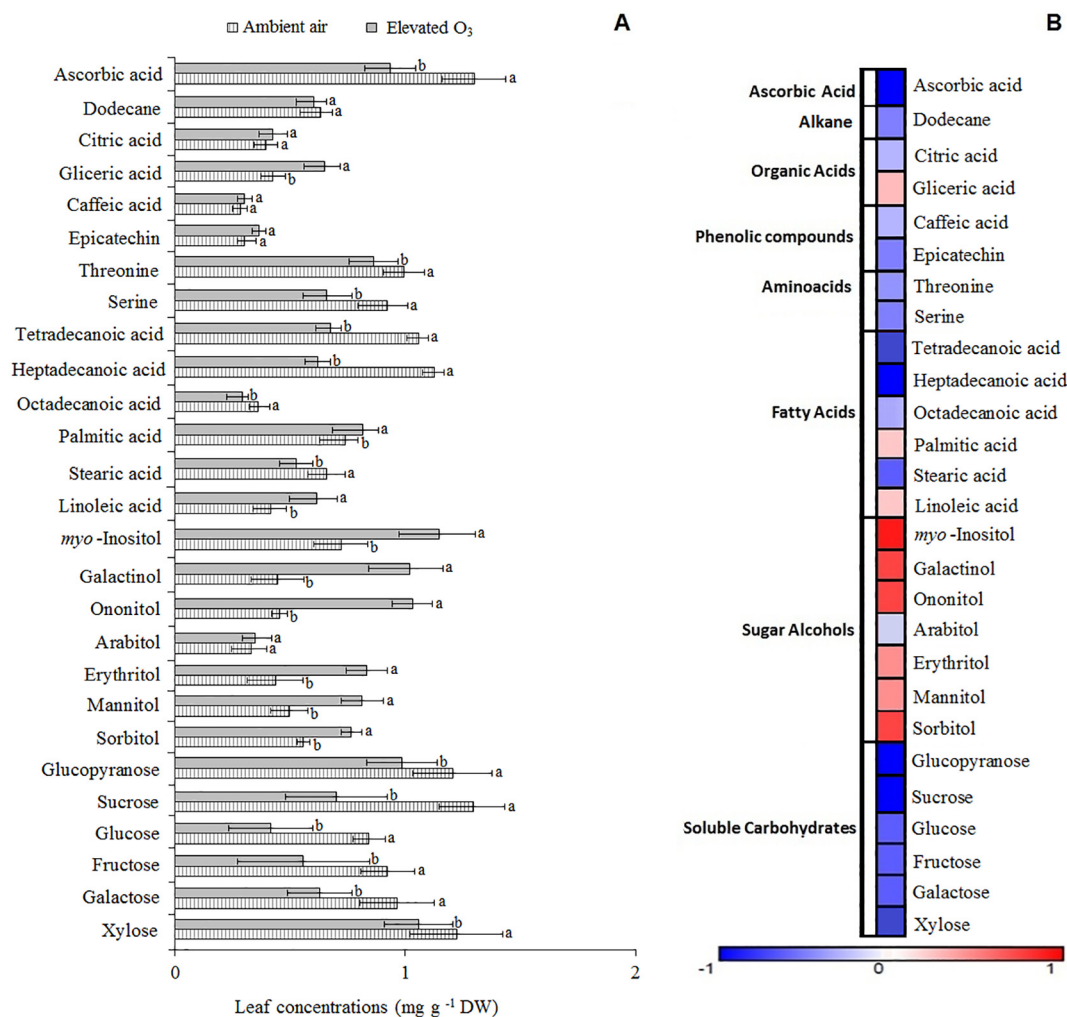


**Fig. 2. A:** Leaf concentrations of major identified compounds by GC-EIMS in *Eugenia uniflora* exposed to two treatments of ozone (ambient air and elevated O<sub>3</sub>). The bars represent mean ± S.E. Different letters indicate significant difference between treatments ( $p < 0.05$ , Student's *t*-test,  $n = 3$  plots). **B:** Heatmap of variations of primary metabolites. Ratios varied from -1 - proportionally lower leaf concentration in plants from elevated O<sub>3</sub> than in those from ambient air- to 1 - proportionally higher leaf concentration in elevated O<sub>3</sub> than in ambient air and are represented by blue and red shades, respectively. (For interpretation of the references to color in this figure legend, the reader is referred to the web version of this article.)

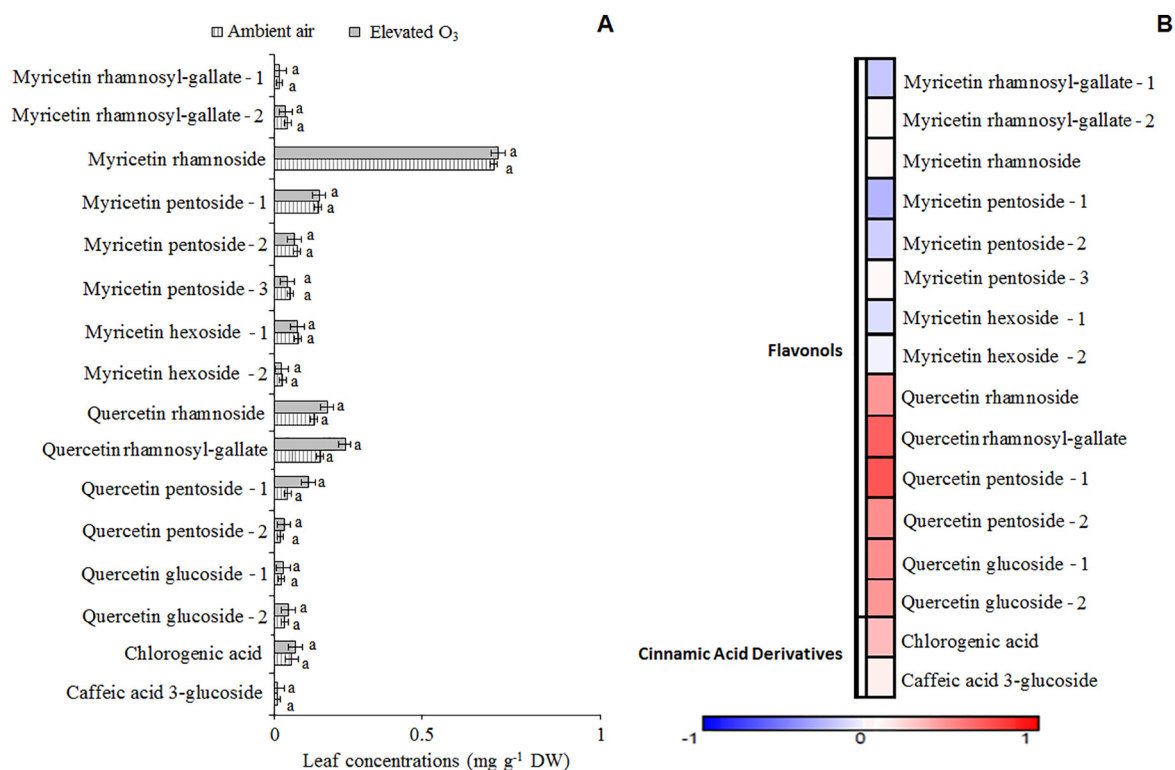


**Fig. 3.** A. Leaf concentrations of phenolic compounds identified by HPLC-MS/MS in *Eugenia uniflora* exposed to two treatments of ozone (ambient air and elevated O<sub>3</sub>). The bars represent mean  $\pm$  S.E. Equal letters indicate non-significant differences between treatments ( $p > 0.05$ , Student's  $t$ -test,  $n = 3$  plots). B. Heatmap of variations of phenolic compounds. Ratios varied from  $-1$  - proportionally lower leaf concentration in plants from elevated O<sub>3</sub> than in those from ambient air - to  $1$  - proportionally higher leaf concentration in elevated O<sub>3</sub> than in ambient air - and are represented by blue and red shades, respectively. (For interpretation of the references to color in this figure legend, the reader is referred to the web version of this article.)

#### 3.4. Parametrization of stomatal conductance model and phytotoxic ozone dose (POD)

The parameterization of stomatal conductance allowed to estimate a  $g_{\max}$  value was of  $82 \text{ mmol O}_3 \text{ m}^{-2} \text{ PLA s}^{-1}$  (Table 2). The value of  $f_{\min}$  was 12% of  $g_{\max}$ . The stomatal light response followed a typical light-response curve, with a light saturation point above  $1000 \mu\text{mol m}^{-2} \text{ s}^{-1}$  (Fig. S3A), while  $g_{\text{SO}_3}$  decreased linearly with increasing O<sub>3</sub> concentration (Fig. S3B). The variation of  $g_{\text{SO}_3}$  with temperature indicated an optimal temperature of 22 °C for stomatal opening (Fig. S3C). More than 1.2 kPa of VPD induced stomatal closure (Fig. S3D). The model estimation of  $g_{\text{SO}_3}$  showed good agreement with the measurement values (Fig. S4) as the model was able to explain 42% of the observed  $g_{\text{SO}_3}$  variance.

The POD0 values were  $3.6 \text{ mmol m}^{-2}$  at ambient air and  $4.7 \text{ mmol m}^{-2}$  at elevated O<sub>3</sub> during the experimental period.

#### 4. Discussion

Exposure to elevated O<sub>3</sub> induced evident alterations in the concentrations of primary metabolites in leaves of *E. uniflora*. The low levels of soluble carbohydrates observed in plants exposed to elevated O<sub>3</sub> may compromise tissue repairing, enzymatic and non-enzymatic antioxidant production and growth (Bäck et al., 1999; Asada, 2006; Nishizawa et al., 2008), as observed in the present study.

The decrease in soluble carbohydrates seems to explain the increased leaf contents of sugar alcohols measured in *E. uniflora* exposed to elevated O<sub>3</sub>, which may be a response of increasing resistance to oxidative stress according to Pedreschi et al. (2009) and Benjamin et al. (2018). It is known that *myo*-inositol, a polyol found in high levels in fumigated plants of *E. uniflora*, alleviates the effects of ROS (Smirnov and Cumbes, 1989; Hu et al., 2018). Also, compounds derived from *myo*-inositol participate in cellular processes in plants, such as signal

transduction and stress tolerance (Melo et al., 2007; Thole and Nielsen, 2008; Okada and Ye, 2009).

On the other hand, the reduction of fatty acid contents in plants growing under high O<sub>3</sub> concentrations is an indication of a reduced antioxidant ability of *E. uniflora*, since high contents of unsaturated fatty acids exerts an antioxidant role, favoring physiological processes of defense against free radicals (Mueller et al., 2006; Tsaluchidu et al., 2008; Yu et al., 2019).

Surprisingly, the polyphenol profile of *E. uniflora* did not change in response to elevated O<sub>3</sub>, despite its known constitutive metabolic diversity (Kade et al., 2008; Mesquita et al., 2017; Souza et al., 2018). The major flavonoid constituent of this species was myricetin rhamnoside, which has a lower antioxidant efficiency than quercetin derivatives (Agati et al., 2012; Ruiz-Cruz et al., 2017). Therefore, the polyphenol profile, although diverse, seemed less efficient as ROS scavenger than expected.

The inefficient antioxidant responses indicated by the reduction of enzymatic and non-enzymatic compounds also revealed that *E. uniflora* was not able to compensate the oxidative stress caused by elevated O<sub>3</sub> levels. The lower detoxification capacity is also confirmed by the fact that photosynthetic damage per unit of O<sub>3</sub> uptake was rather high in this species. In fact, even though POD0 values were low and visible foliar injuries were not observed, deleterious O<sub>3</sub> impacts on photosynthesis were found in *E. uniflora*. In addition to high stomatal defense capacity, we postulate that the constitutive high content of flavonoids and enhanced levels of sugar alcohols may restrict the appearance of leaf injury, as proposed by Hernández et al. (2009).

Increased ROS concentrations inside the cells cause membrane damage (lipid peroxidation), protein oxidation, RNA and DNA degradation, chlorophyll bleaching, and eventually lead to the destruction of the cells (Vaultier and Jolivet, 2015; Choudhury et al., 2017; Yadav et al., 2019). In this study, the higher occurrence of lipid peroxidation -

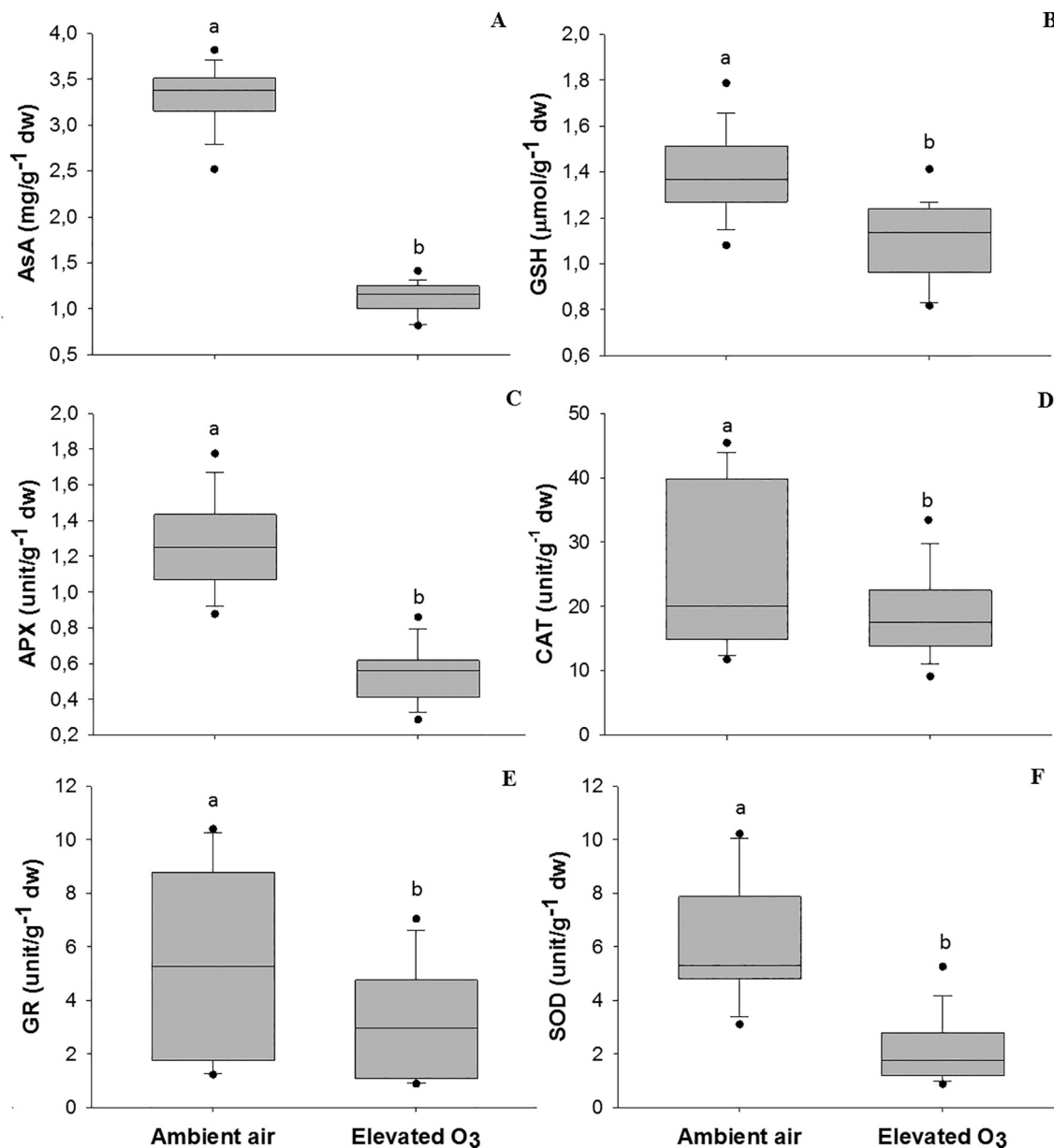


**Fig. 4.** Concentrations of non-enzymatic compounds: (A) ascorbic acid (AsA) and (B) glutathione (GSH); and activities of enzymatic compounds: (C) ascorbate peroxidase (APX), (D) catalase (CAT), (E) glutathione reductase (GR), and (F) superoxide dismutase (SOD) in leaves of *Eugenia uniflora* exposed to ambient air and elevated ozone  $O_3$ . Box plots show median, 25%, 75%-percentile, maximum, minimum of values. Distinct lowercase letters indicate significant differences between treatments, ( $p < 0.05$ , Student's  $t$ -test,  $n = 3$  plots).

measured by the contents of MDA and HPCD - under elevated  $O_3$ , together with inefficient antioxidant metabolism of ascorbate-glutathione cycle, low stomatal conductance, and reduced growth in height, corroborate the assumption that *E. uniflora* is sensitive to elevated  $O_3$  levels, contradicting the initial hypothesis. The growth and biomass allocation to different organs were altered in *E. uniflora* plants, as mentioned by several authors (Wittig et al., 2009; Moura et al., 2018; Hoshika et al., 2020).  $O_3$  induced some alterations in biomass partitioning between above and below organs, resulting in reduced root/shoot ratio, even though 75 days of  $O_3$  exposure may not be sufficient to accumulate significant effects on tree biomass. *E. uniflora* exposed to elevated  $O_3$  presented an accelerated leaf turnover compared to plants exposed to ambient air, as also observed in *Alnus glutinosa* and sugarcane genotype IACSP95-5000 by Hoshika et al. (2020) and Moura et al. (2018), respectively. The leaf turnover is an important process to compensating the decline of photosynthetic rate and support the mobilization of reserves (Hikosaka, 2004; Falster et al., 2018).

This species showed no leaf visible injury even after 75 days of  $O_3$  exposure (data not shown). The flux-based approach may provide a proper assessment of  $O_3$  injury to plants (Hoshika et al., 2020). Sicard et al. (2016) and Hoshika et al. (2018) suggested flux-based critical levels against leaf visible injury of 20–25  $mmol m^{-2} POD_0$  for forest trees. However, only a few studies had been reported for modelling stomatal  $O_3$  flux in tropical forest trees (Cassimiro et al., 2016). To calculate  $POD_0$ , we provided for the first time the parameterization of the stomatal conductance model in *E. uniflora*. As a result, the absence of visible foliar injury in *E. uniflora* may be associated with low stomatal conductance ( $g_{max} = 82 mmol O_3 m^{-2} PLA s^{-1}$ ) and  $O_3$ -induced stomatal closure ( $f_{O_3}$ ) which may restrict stomatal  $O_3$  uptake, thus limiting possible  $O_3$  damages (Hoshika et al., 2020c). In fact, *E. uniflora* leaves had lower  $POD_0$  values than the critical levels for visible foliar  $O_3$  injury even under elevated  $O_3$  ( $POD_0 = 4.7 mmol m^{-2}$ ). Interestingly,  $POD_0$  at elevated  $O_3$  was just 30% higher than at ambient, although twice higher mean  $O_3$  concentrations were observed in elevated  $O_3$ .

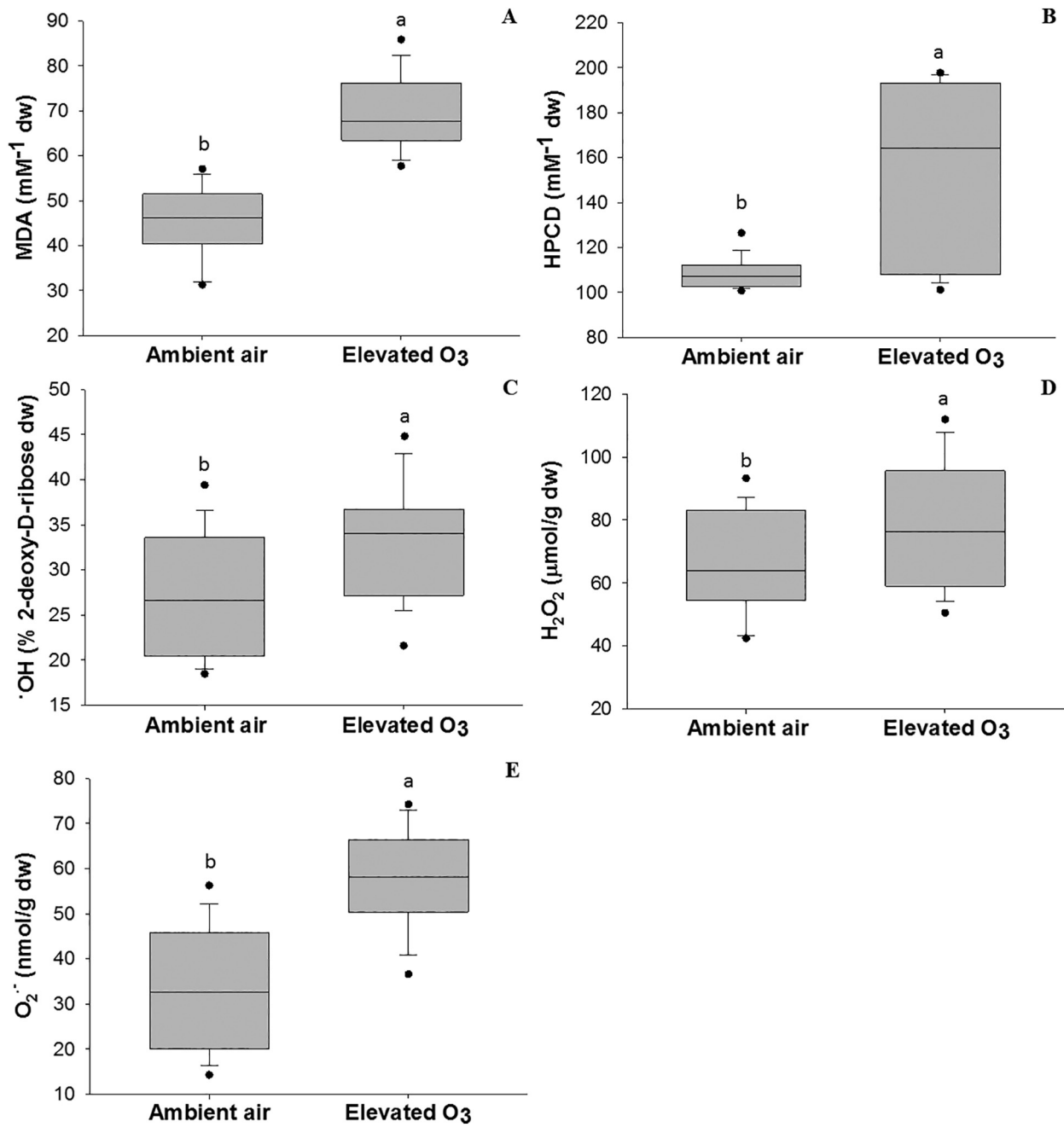


**Fig. 5.** Indicators of lipid peroxidation: (A) malondialdehyde (MDA) and (B) hydroperoxide conjugated diene (HPCD); and concentration of reactive oxygen species: (C) hydroxyl radical (OH<sup>·</sup>), (D) hydrogen peroxide (H<sub>2</sub>O<sub>2</sub>), (E) and superoxide radical (O<sub>2</sub><sup>·-</sup>), in leaves of *Eugenia uniflora* exposed to ambient air and elevated O<sub>3</sub>. Box plots show median, 25%-, 75%-percentile, maximum, minimum of values. Distinct lowercase letters indicate significant differences between treatments ( $p < 0.05$ , Student's  $t$ -test,  $n = 3$  plots).

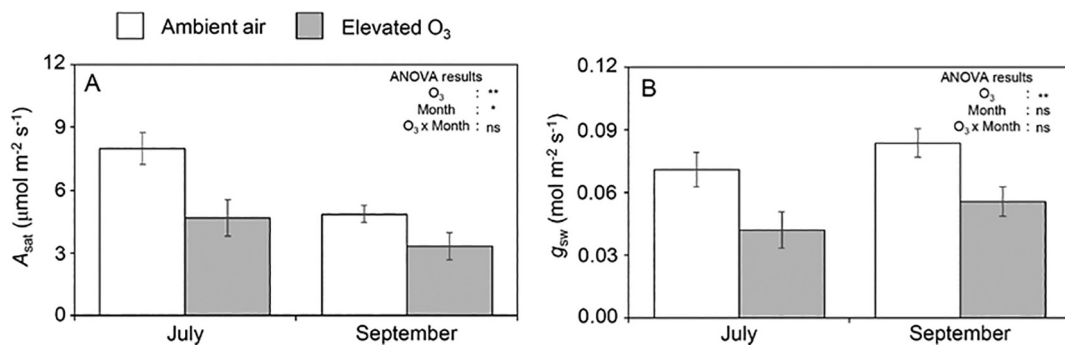


**Fig. 6.** Net photosynthetic rate ( $A_{sat}$ ) and stomatal conductance ( $g_{sw}$ ) of *Eugenia uniflora* in July and September 2017 under two levels of O<sub>3</sub> (ambient air and elevated O<sub>3</sub>). The bars represent mean ± S.E. ( $n = 3$  plots). Two-way ANOVA: \* $p < 0.05$ , \*\* $p < 0.01$ , ns denotes not significant.



**Table 1**

Leaf, stem and root biomass (g), root/shoot ratio, height (cm), stem diameter (cm) and number of leaves of *E. uniflora* exposed to two O<sub>3</sub> treatments (ambient air and elevated O<sub>3</sub>) for 75 days. Data are shown as mean ± S.E. Distinct lowercase letters indicate significant differences between treatments (p < 0.05, Student's *t*-test, n = 3 plots).

Parameters	Ambient air	Elevated O <sub>3</sub>
Biomass		
Leaves	0.67 ± 0.08 b	1.47 ± 0.06 a
Stems	2.09 ± 0.10 a	2.22 ± 0.09 a
Roots	2.57 ± 0.20 a	2.20 ± 0.20 a
Root/shoot ratio	1.16 ± 0.07 a	0.89 ± 0.05 b
Growth		
Height	37.85 ± 0.91 a	34.20 ± 0.92 b
Stem diameter	5.53 ± 0.14 a	5.94 ± 0.19 a
Leaf number	65.16 ± 6.28 b	83.05 ± 4.30 a

## 5. Conclusions

The whole set of results led us to reject the proposed hypothesis and assume that *E. uniflora* plants are sensitive to O<sub>3</sub>, although visible foliar injury did not occur. POD0 values were lower than the critical levels for visible foliar O<sub>3</sub> injury reported in the literature, as a result of low stomatal conductance observed for this species.

The hypothesis rejection was based on the following findings: reduction in soluble carbohydrates and fatty acid contents; non-significant changes in the polyphenol profile, despite its constitutive diversity, mainly regarding flavonols that are powerful antioxidants; inefficient antioxidant responses associated to the ascorbate-glutathione cycle, as indicated by the reduction of enzymatic and non-enzymatic compounds; increased contents of ROS and lipid peroxidation indicators; reduction in net photosynthesis and stomata conductance; growth reduction and reduced root to shoot ratio.

## CRedit authorship contribution statement

Elena Paoletti, Marisa Domingos and Claudia Maria Furlan planned the experiment. Marcela Regina Gonçalves da Silva Engela, Marisia Pannia Esposito, Francine Faia Fernandes, Yasutomo Hoshika and Elisa Carrari carried out the experiment. Marcela Regina Gonçalves da Silva Engela and Marisia Pannia Esposito led the writing of the manuscript. All authors provided critical feedback and helped shape the research, analysis and manuscript.

## Declaration of competing interest

The authors declare that they have no known competing financial interests or personal relationships that could have appeared to influence the work reported in this paper.

**Table 2**

Stomatal conductance model parameters estimated for *Eugenia uniflora*.  $g_{\max}$  is maximum stomatal conductance,  $f_{\min}$  is minimum stomatal conductance,  $a$  is a parameter determining the shape of the hyperbolic relationship of  $g_{sO_3}$  response to light,  $b$  is a parameter to describe the variation of  $g_{sO_3}$  with O<sub>3</sub> concentration,  $T_{\max}$ ,  $T_{opt}$  and  $T_{\min}$  are maximum, optimal and minimum temperature for stomatal opening,  $VPD_{\min}$  and  $VPD_{\max}$  are the vapor pressure deficit for attaining minimum and maximum stomatal aperture ( $f_{VPD}$ ).

Stomatal conductance model parameters		<i>E. uniflora</i>
$g_{\max}$	(mmol O <sub>3</sub> m <sup>-2</sup> PLA s <sup>-1</sup> )	82
$f_{\min}$	(Fraction)	0.12
$f_{light}$	$a$ (Constant)	0.0033
$f_{O_3}$	$b$ (Constant)	0.0039
$f_{temp}$	$T_{opt}$ (°C)	22
	$T_{\min}$ (°C)	4
	$T_{\max}$ (°C)	50
$f_{VPD}$	$VPD_{\max}$ (kPa)	1.2
	$VPD_{\min}$ (kPa)	6.6

## Acknowledgments

The authors thank the financial support provided by Fundação de Desenvolvimento da Pesquisa do Agronegócio (FUNDEPAG), Conselho Nacional de Desenvolvimento Científico e Tecnológico (CNPq), the Fondazione Cassa di Risparmio di Firenze (2013/7956) and the LIFE15 ENV/IT/000183 project MOTTLES. We also thank the Companhia Energética de São Paulo (CESP), for donating the *Eugenia uniflora* plants, Alessandro Materassi for design and maintenance of the ozone FACE, Moreno Lazzara for assistance during the field work, Mourisa Ferreira and Aline Bertinato Cruz for assistance with analyzes on GC-MS and HPLC, and Pamela Tavares for help with Heatmap analysis.

## Appendix A. Supplementary data

Supplementary data to this article can be found online at <https://doi.org/10.1016/j.scitotenv.2021.145080>.

## References

- Agathokleous, E., Feng, Z., Oksanen, E., Sicard, P., Wang, Q., Saitanis, C.J., Araminiene, V., Blande, J.D., Hayes, F., Calatayud, V., Domingos, M., Veresoglou, S.D., Peñuelas, J., Wardle, D.A., De Marco, A., Li, Z., Harmens, H., Yuan, X., Vitale, M., Paoletti, E., 2020. Ozone affects plant, insect, and soil microbial communities: a threat to terrestrial ecosystems and biodiversity. *Sci. Adv.* 6 (33), eabc1176. <https://doi.org/10.1126/sciadv.abc1176>.
- Agati, G., Azzarello, E., Pollastri, S., Tattini, M., 2012. Flavonoids as antioxidants in plants: location and functional significance. *Plant Sci.* 196, 67–76. <https://doi.org/10.1016/j.plantsci.2012.07.014>.
- Aguiar-Silva, C., Brandão, S.E., Domingos, M., Bulbovas, P., 2016. Antioxidant responses of Atlantic Forest native tree species as indicators of increasing tolerance to oxidative stress when they are exposed to air pollutants and seasonal tropical climate. *Ecol. Indic.* 63, 154–164. <https://doi.org/10.1016/j.ecolind.2015.11.060>.
- Alexieva, V., Sergiev, I., Mapelli, S., Karanov, E., 2001. The effect of drought and ultraviolet radiation on growth and stress markers in pea and wheat. *Plant Cell Environ.* 24, 1337–1344. <https://doi.org/10.1046/j.1365-3040.2001.00778.x>.
- Alonso, R., Elvira, S., Sanz, M.J., Gerosa, G., Emberson, L.D., Bermejo, B., Gimeno, B.S., 2008. Sensitivity analysis of a parameterization of the stomatal component of the DO<sub>3</sub>SE model for *Quercus ilex* to estimate ozone fluxes. *Environ. Pollut.* 155, 473–480. <https://doi.org/10.1016/j.envpol.2008.01.032>.
- Asada, K., 2006. Production and scavenging of reactive oxygen species in chloroplasts and their functions. *Plant Physiol.* 141 (2), 391–396. <https://doi.org/10.1104/pp.106.082040>.
- Auricchio, M.T., Bacchi, E.M., 2003. Folhas de *Eugenia uniflora* L. (pitanga): propriedades farmacobotânicas, químicas e farmacológicas. *Rev. Inst. Adolfo Lutz* 62 (1), 55–61.
- Azevedo, R.A., Alas, R.M., Smith, R.J., Lea, P.J., 1998. Response of antioxidant enzymes to transfer from elevated carbon dioxide to air and ozone fumigation in the leaves and roots of wild-type and a catalase deficient mutant of barley. *Physiol. Plant.* 104 (2), 280–292. <https://doi.org/10.1034/j.1399-3054.1998.1040217.x>.
- Bäck, J., Vanderklein, D.W., Topa, M.A., 1999. Effects of elevated ozone on CO<sub>2</sub> uptake and leaf structure in sugar maple under two light environments. *Plant Cell Environ.* 22, 137–147. <https://doi.org/10.1046/j.1365-3040.1999.00393.x>.
- Benjamin, J.J., Lucini, L., Jothiramshekar, S., Parida, A., 2018. Metabolomic insights into the mechanisms underlying tolerance to salinity in different halophytes. *Plant Physiol. Biochem.* <https://doi.org/10.1016/j.plaphy.2018.11.006>.
- Bičárová, S., Sitková, Z., Pavlendová, H., Fleisher Jr., P., Fleisher Sr., P., Bytnerowicz, A., 2019. The role of environmental factors in ozone uptake of *Pinus mugo* Turra. *Atmos. Pollut. Res.* 10, 283–293. <https://doi.org/10.1016/j.apr.2018.08.003>.
- Bloss, W., 2018. Measurement of air pollutants. Reference module in earth systems and environmental sciences. *Encyclopedia of Environmental Health*, 2, pp. 1–11. <https://doi.org/10.1016/B978-0-12-409548-9.11354-5>.
- Booker, F., Burkey, K., Morgan, P., Fiscus, E., Jones, A., 2012. Minimal influence of G-protein null mutations on ozone-induced changes in gene expression, foliar injury, gas exchange and peroxidase activity in *Arabidopsis thaliana* L. *Plant Cell Environ.* 35, 668–681. <https://doi.org/10.1111/j.1365-3040.2011.02443.x>.
- Brandão, S.E., Bulbovas, P., Lima, M.E., Domingos, M., 2017. Biochemical leaf traits as indicators of tolerance potential in tree species from the Brazilian Atlantic Forest against oxidative environmental stressors. *Sci. Total Environ.* 575, 406–417. <https://doi.org/10.1016/j.scitotenv.2016.10.006>.
- Braun, S., Schindler, C., Leuzinger, S., 2010. Use of sap flow measurements to validate stomatal functions for mature beech (*Fagus sylvatica*) in view of ozone uptake calculations. *Environ. Pollut.* 158, 2954–2963. <https://doi.org/10.1016/j.envpol.2010.05.028>.
- Cardoso-Gustavson, P., Moura, B.B., Fernandes, F.F., Dias, M.G., Pedrosa, G.S., Souza, S.R., Paoletti, E., Domingos, M., 2020. Alternative routes for ozone uptake and damage in the leaf structure of tropical plants. In: Agrawal, S.B., Agrawal, M., Singh, A. (Eds.), *Tropospheric Ozone: A Hazard for Vegetation and Human Health*. Cambridge Scholars Publishing, United Kingdom (In press).
- Cassimiro, J.C., Moura, B.B., Alonso, R., Meirelles, S.T., Moraes, R.M., 2016. Ozone stomatal flux and O<sub>3</sub> concentration-based metrics for *Astronium graveolens* Jacq., a Brazilian native forest tree species. *Environ. Pollut.* 213, 1007–1015.

- Choudhury, F.K., Rivero, R.M., Blumwald, E., Mittler, R., 2017. Reactive oxygen species, abiotic stress and stress combination. *Plant J.* 90, 856–867. <https://doi.org/10.1111/tpj.13299>.
- CLRTAP, 2017. Mapping critical levels for vegetation, chapter III of manual on methodologies and criteria for modelling and mapping critical loads and levels and air pollution effects, risks and trends. UNECE Convention on Long-Range Transboundary Air Pollution; Accessed on 27 March 2019 on Web at [www.icpmapping.org](http://www.icpmapping.org).
- Da Cunha, F.A.B., Waczuk, E.P., Duarte, A.E., Barros, L.M., Elekofehinti, O.O., Matias, E.F.F., Da Costa, J.G.M., Sanmi, A.A., Boligon, A.A., Rocha, J.B.T., Souza, D.O., Posser, T., Coutinho, H.D.M., Franco, J.L., Kamdem, J.P., 2016. Cytotoxic and antioxidative potentials of ethanolic extract of *Eugenia uniflora* L. (Myrtaceae) leaves on human blood cells. *Biomed. Pharmacother.* 84, 614–621. <https://doi.org/10.1016/j.biopha.2016.09.089>.
- Denardin, C.C., Hirsch, G.E., Rocha, R.F., Vizzotto, M., Henriques, A.T., Moreira, J.C.F., Guma, F.T.C.R., Emanuelli, T., 2015. Antioxidant capacity and bioactive compounds of four Brazilian native fruits. *J. Food Drug Anal.* 23, 387–398. <https://doi.org/10.1016/j.jfda.2015.01.006>.
- Domingos, M., Bulbovas, P., Camargo, C.Z.S., Aguiar-Silva, C., Brandão, S.E., D Afré-Martinelli, M., Dias, A.P.L., Engela, M.R.G.S., Gagliano, J., Moura, B.B., Alves, E.S., Rinaldi, M.C.S., Gomes, E.P.C., Furlan, C.M., Figueiredo, A.M.G., 2015. Searching for native tree species and respective potential biomarkers for future assessment of pollution effects on the highly diverse Atlantic Forest in SE-Brazil. *Environ. Pollut.* 202, 85–95. <https://doi.org/10.1016/j.envpol.2015.03.018>.
- Dong, Y., Li, J., Guo, J., Jiang, Z., Chu, Y., Chang, L., Yang, Y., Liao, H., 2020. The impact of synoptic patterns on summertime ozone pollution in the North China Plain. *Sci. Total Environ.* 139559 (735), 1–13. <https://doi.org/10.1016/j.scitotenv.2020.139559>.
- Du, B., Kreuzwieser, J., Winkler, J.B., Ghirardo, A., Schnitzler, J.P., Ache, P., Rennenberg, H., 2018. Physiological responses of date palm (*Phoenix dactylifera*) seedlings to acute ozone exposure at high temperature. *Environ. Pollut.* 242, 905–913. <https://doi.org/10.1016/j.envpol.2018.07.059>.
- Esposito, M.P., Pedrosa, A.N.V., Domingos, M., 2016. Assessing redox potential capacity of a native tree from the Atlantic Rain Forest in SE – Brazil during the exchange of the power generation source of an oil refinery. *Sci. Total Environ.* 550, 861–870. <https://doi.org/10.1016/j.scitotenv.2016.01.196>.
- Esposito, M.P., Nakazato, R.K., Pedrosa, A.N.V.P., Lima, M.E.L., Figueiredo, M.A., Diniz, A.P., Kozovitz, A.R., Domingos, M., 2018. Oxidant-antioxidant balance and tolerance against oxidative stress in pioneer and non-pioneer tree species from the remaining Atlantic Forest. *Sci. Total Environ.* 625, 382–393. <https://doi.org/10.1016/j.scitotenv.2017.12.255>.
- Falster, D.S., Duursma, R.A., Fitz-John, R.G., 2018. How functional traits influence plant growth and shade tolerance across the life cycle. *Proc. Natl. Acad. Sci.* 115 (29), E6789–E6798. <https://doi.org/10.1073/pnas.1714044115>.
- Garmus, T.T., Paviani, L.C., Queiroga, C.L., Magalhães, P.M., Cabral, F.A., 2014. Extraction of phenolic compounds from pitanga (*Eugenia uniflora* L.) leaves by sequential extraction in fixed bed extractor using supercritical CO<sub>2</sub>, ethanol and water as solvents. *J. Supercrit. Fluid.* 86, 4–14. <https://doi.org/10.1016/j.supflu.2013.11.014>.
- Gerken, T., Wei, D., Chase, R.J., Fuentes, J.D., Schumacher, C., Machado, L.A.T., Andreoli, R. V., Chamecki, M., Souza, R.A.F., Freire, L.S., Jardine, A.B., Manzi, A.O., Santos, R.M.N., Randow, C., Costa, S., Stoy, P.C., Tóta, J., Trowbridge, A.M., 2016. Downward transport of ozone rich air and implications for atmospheric chemistry in the Amazon rainforest. *Atmos. Environ.* 124, 64–76.
- Hernández, I., Alegre, L., Van Breusegem, F., Munné-Bosch, S., 2009. How relevant are flavonoids as antioxidants in plants? *Trends Plant Sci.* 14 (3), 125–132. <https://doi.org/10.1016/j.tplants.2008.12.003>.
- Hikosaka, K., 2004. Leaf canopy as a dynamic system: ecophysiology and optimality in leaf turnover. *Ann. Bot.* 95 (3), 521–533. <https://doi.org/10.1093/aob/mci050>.
- Hodges, D.M., DeLong, J.M., Forney, C.F., Prange, R.K., 1999. Improving the thiobarbituric acid-reactive-substances assay for estimating lipid peroxidation in plant tissues containing anthocyanin and other interfering compounds. *Planta* 207, 604–611. <https://doi.org/10.1007/s004250050524>.
- Hoshika, Y., Paoletti, E., Omasa, K., 2012. Parameterization of *Zelkova serrata* stomatal conductance model to estimate stomatal ozone uptake in Japan. *Atmos. Environ.* 55, 271–278. <https://doi.org/10.1016/j.atmosenv.2012.02.083>.
- Hoshika, Y., Carrari, E., Zhang, L., Carriero, G., Pignatelli, S., Fasano, G., Materassi, A., Paoletti, E., 2018. Testing a ratio of photosynthesis to O<sub>3</sub> uptake as an index for assessing O<sub>3</sub>-induced foliar visible injury in poplar trees. *Environ. Sci. Pollut. Res. Int.* 25, 8113–8124. <https://doi.org/10.1007/s11356-017-9475-6>.
- Hoshika, Y., Fares, S., Pellegrini, E., Conte, A., Paoletti, E., 2020. Water use strategy affects avoidance of ozone stress by stomatal closure in Mediterranean trees - a modelling analysis. *Plant Cell Environ.* 43, 611–623. <https://doi.org/10.1111/pce.13700>.
- Hoshika, Y., Paoletti, E., Agathokleous, E., Sugai, T., Koike, T., 2020c. Developing ozone risk assessment for larch species. *Front. For. Glob. Change.* 3, 45. <https://doi.org/10.3389/ffgc.2020.00045>.
- Hu, L., Zhou, K., Li, Y., Chen, X., Liu, B., Li, C., Gong, X., Ma, F., 2018. Exogenous myo-inositol alleviates salinity-induced stress in *Malus hupehensis* Rehd. *Plant Physiol. Biochem.* 133, 116–126. <https://doi.org/10.1016/j.plaphy.2018.10.037>.
- Israr, M., Sahi, S., Datta, R., Sarkar, D., 2006. Bioaccumulation and physiological effects of mercury in *Sesbania drummondii*. *Chemosphere* 591–598 (126), 65. <https://doi.org/10.1016/j.chemosphere.2006.02.016>.
- Kade, I.J., Ibukun, E.O., Nogueira, C.W., Rocha, J.B., 2008. Sun-drying diminishes the antioxidative potentials of leaves of *Eugenia uniflora* against formation of thiobarbituric acid reactive substances induced in homogenates of rat brain and liver. *Exp. Toxicol. Pathol.* 60 (4–5), 365–371. <https://doi.org/10.1016/j.etp.2007.12.001>.
- Kraus, T.E., Evans, R.C., Fletcher, R.A., Paul, S.K.P., 1995. Paclitaxel enhances tolerance to increased levels of UV-B radiation in soybean (*Glycine max*) seedlings. *Can. J. Bot.* 73 (6), 797–806. <https://doi.org/10.1139/b95-088>.
- Landi, M., 2017. Commentary to: “improving the thiobarbituric acid-reactive-substances assay for estimating lipid peroxidation in plant tissues containing anthocyanin and other interfering compounds”. *Planta* 245 (6), 1097. <https://doi.org/10.1007/s00425-017-2699-3>.
- Levin, A.G., Pignata, M.L., 1995. *Ramalina ecklonii* as a bioindicator of atmospheric pollution in Argentina. *Can. J. Bot.* 73, 1196–1202. <https://doi.org/10.1139/b95-129>.
- Li, P., Feng, Z., Catalayud, V., Yuan, X., Xu, Y., Paoletti, E., 2017. A meta-analysis on growth, physiological, and biochemical responses of woody species to ground-level ozone highlights the role of plant functional types. *Plant Cell Environ.* 40, 2369–2380.
- Li, M., Dong, H., Wang, B., Zhao, W., Sakthividi, J.V.Z., Li, L., Lin, C., Yang, Y., 2020. Association between ambient ozone pollution and mortality from a spectrum of causes in Guangzhou, China. *Sci. Total Environ.* 142110. <https://doi.org/10.1016/j.scitotenv.2020.142110>.
- Lopes, G.K.B., Schulman, H.M., Hermes-Lima, M., 1999. Polyphenol tannic acid inhibits hydroxyl radical formation from Fenton reaction by complexing ferrous ions. *Biochim. Biophys. Acta* 1472, 142–152. [https://doi.org/10.1016/S0304-4165\(99\)00117-8](https://doi.org/10.1016/S0304-4165(99)00117-8).
- López, A., Montaña, A., García, P., Garrido, A., 2005. Note: quantification of ascorbic acid and dehydroascorbic acid in fresh olives in commercial presentations of table olives. *Food Sci. Technol. Int.* 11 (3), 199–204. <https://doi.org/10.1177/1082013205054421>.
- Melo, R.M., Corrêa, V.F.S., Amorim, A.C.L., Miranda, A.L.P., Rezende, C.M., 2007. Identification of impact aroma compounds in *Eugenia uniflora* L. (Brazilian Pitanga) leaf essential oil. *J. Braz. Chem. Soc.* 18 (1), 179–183. <https://doi.org/10.1590/s0103-50532007000100020>.
- Mesquita, P.R.R., Nunes, E.C., Santos, F.N., dos Bastos, L.P., Costa, M.A.P.C., de M. Rodrigues, F., De Andrade, J.B., 2017. Discrimination of *Eugenia uniflora* L. biotypes based on volatile compounds in leaves using HS-SPME/GC–MS and chemometric analysis. *Microchem. J.* 130, 79–87. <https://doi.org/10.1016/j.microc.2016.08.005>.
- Mierziak, J., Kostyn, K., Kulma, A., 2014. Flavonoids as important molecules of plant interactions with the environment. *Molecules* 19, 16240–16265. <https://doi.org/10.3390/molecules191016240>.
- Moura, B.B., Hoshika, Y., Ribeiro, R.V., Paoletti, E., 2018. Exposure- and flux-based assessment of ozone risk to sugarcane plants. *Atmos. Environ.* 176, 252–260. <https://doi.org/10.1016/j.atmosenv.2017.12.039>.
- Mouradov, A., Spangenberg, G., 2014. Flavonoids: a metabolic network mediating plants adaptation to their real estate. *Front. Plant Sci.* 5, 1–16. <https://doi.org/10.3389/fpls.2014.00620>.
- Mueller, M.J., Mène-Saffrané, L., Grun, C., Karg, K., Farmer, E.E., 2006. Oxylipin analysis methods. *Plant J.* 45 (4), 472–489. <https://doi.org/10.1111/j.1365-313X.2005.02614.x>.
- Nishizawa, A., Yabuta, Y., Shigeoka, S., 2008. Galactinol and raffinose constitute a novel function to protect plants from oxidative damage. *Plant Physiol.* 147 (3), 1251–1263. <https://doi.org/10.1104/pp.108.122465>.
- Okada, M., Ye, K., 2009. Nuclear phosphoinositide signaling regulates messenger RNA export. *RNA Biol.* 6, 12–16. <https://doi.org/10.4161/rna.6.1.7439>.
- Oue, H., Motohiro, S., Inada, K., Miyata, A., Mano, M., Kobayashi, K., Zhu, J., 2008. Evaluation of ozone uptake by the rice canopy with the multi-layer model. *J. Agric. Meteorol.* 64, 223–232. <https://doi.org/10.2480/agrmet.64.4.8>.
- Paoletti, E., Materassi, A., Fasano, G., Hoshika, Y., Carriero, G., Silaghi, D., Badae, O., 2017. A new-generation 3D ozone FACE (free air controlled exposure). *Sci. Total Environ.* 575, 1407–1414. <https://doi.org/10.1016/j.scitotenv.2016.09.217>.
- Paralovo, S.L., Barbosa, C.G.G., Carneiro, I.P.S., Kurzlop, P., Borillo, G.C., Schiochet, M.F.C., Godoi, R.H.M., Yamamoto, C.L., Souza, R.A.F., Andreoli, R.V., Ribeiro, I.O., Manzi, A.O., Kourtchev, I., Bustillos, J.O.V., Martin, S.T., Godoi, R.H.M., 2019. Observations of particulate matter, NO<sub>2</sub>, SO<sub>2</sub>, O<sub>3</sub>, H<sub>2</sub>S and selected VOCs at a semi-urban environment in the Amazon region. *Sci. Total Environ.* 650, 996–1006. <https://doi.org/10.1016/j.scitotenv.2018.09.073>.
- Pedreschi, R., Franck, C., Lammertyn, J., Erban, A., Kopka, J., Hertog, M., Nicolai, B., 2009. Metabolic profiling of “conference” pears under low oxygen stress. *Postharvest Biol. Tec.* 51 (2), 123–130. <https://doi.org/10.1016/j.postharvbio.2008.05.019>.
- Peshev, D., Van den Ende, W., 2013. Sugars as antioxidants in plants. In: Tuteja, N., Gill, S.S. (Eds.), *In Crop Improvement under Adverse Conditions*. Springer-Verlag, Berlin, Heidelberg, Germany, pp. 285–308.
- Pope, R.J., Arnold, S.R., Chipperfield, M.P., Reddington, C.L.S., Butt, E.W., Keslake, T.D., Feng, W., Latter, B.G., Kerridge, B.J., Siddans, R., Rizzo, L., Artaxo, P., Sadiq, M., Tai, A.P.K., 2019. Substantial increases in Eastern Amazon and Cerrado biomass burning-sourced tropospheric ozone. *Geophys. Res. Lett.* 46, 1–22. <https://doi.org/10.1029/2019GL084143>.
- Reddy, A.R., Chaitanya, K.V., Jutur, P.P., Sumithra, K., 2004. Differential antioxidative responses to water stress among five mulberry (*Morus alba* L.) cultivars. *Environ. Exp. Bot.* 52 (1), 33–42. <https://doi.org/10.1016/j.envexpbot.2004.01.002>.
- Richet, N., Tozo, K., Afif, D., Banvoy, J., Legay, S., Dizengremel, P., Cabané, M., 2012. The response to daylight or continuous ozone of phenylpropanoid and lignin biosynthesis pathways in poplar differs between leaves and wood. *Planta* 236 (2), 727–737. <https://doi.org/10.1007/s00425-012-1644-8>.
- Ruiz-Cruz, S., Chaparro-Hernández, S., Ruiz, K.L.H., Cira-Chávez, L.A., Estrada-Alvarado, M. I., Ortega, L.E.G., Mata, M.A.L., 2017. Flavonoids: important biocompounds in food. In: Justino, G. (Ed.), *Flavonoids - From Biosynthesis to Human Health*, London, pp. 353–369. <https://doi.org/10.5772/67864>.
- Sá, A.F.L., Valeri, S.V., Cruz, M.C.P., Barbosa, J.C., Rezende, G.M., Teixeira, M.P., 2014. Effects of potassium application and soil moisture on the growth of *Corymbia citriodora* plants. *Cerne* 20, 645–651. <https://doi.org/10.1590/01047760201420041422>.
- Shu, X., Zhang, Y., Jia, J., Ren, X., Wang, Y., 2019. Extraction, purification and properties of water-soluble polysaccharides from mushroom *Lepista nuda*. *Int. J. Biol. Macromol.* 128, 858–869. <https://doi.org/10.1016/j.ijbiomac.2019.01.024>.
- Sicard, P., De Marco, A., Dalstein-Richier, L., Tagliarferro, F., Renou, C., Paoletti, E., 2016. An epidemiological assessment of stomatal ozone flux-based critical levels for visible ozone injury in Southern European forests. *Sci. Total Environ.* 541, 729–741. <https://doi.org/10.1016/j.scitotenv.2015.09.113>.
- Siciliano, B., Dantas, G., da Silva, C.M., Arbilla, G., 2020. Increased ozone levels during the COVID-19 lockdown: analysis for the city of Rio de Janeiro, Brazil. *Sci. Total Environ.* 139765 (737), 1–8. <https://doi.org/10.1016/j.scitotenv.2020.139765>.

- Smirnoff, N., Cumbes, Q., 1989. Hydroxyl radical scavenging activity of compatible solutes. *Phytochemistry* 28, 1057–1060. [https://doi.org/10.1016/0031-9422\(89\)80182.7](https://doi.org/10.1016/0031-9422(89)80182.7).
- Sobeh, M., El-Raey, M., Rezaq, S., Abdelfattah, M.A.O., Petruk, G., Osman, S., El-Shazly, A.M., El-Beshbishy, H.A., Mahmoud, M.F., Wink, M., 2019. Chemical profiling of secondary metabolites of *Eugenia uniflora* and their antioxidant, anti-inflammatory, pain killing and anti-diabetic activities: a comprehensive approach. *J. Ethnopharmacol.* 240 (111939), 1–12. <https://doi.org/10.1016/j.jep.2019.111939>.
- Souza, L., Silva-Rocha, W., Ferreira, M., Soares, L., Svidzinski, T., Milan, E., Pires, R.H., Almeida, A.M.F., Mendes-Giannini, M.J.S., Chaves, G.M., 2018. Influence of *Eugenia uniflora* extract on adhesion to human Buccal epithelial cells, biofilm formation, and cell surface hydrophobicity of *Candida* spp. from the oral cavity of kidney transplant recipients. *Molecules* 23 (10), 2418. <https://doi.org/10.3390/molecules23102418>.
- Suguiyama, V.F., Silva, E.A., Meirelles, S.T., Centeno, D.C., Braga, M.R., 2014. Leaf metabolite profile of the Brazilian resurrection plant *Barbacenia purpurea* Hook. (Velloziaceae) shows two time-dependent responses during desiccation and recovering. *Front. Plant Sci.* 5, 1–14. <https://doi.org/10.3389/fpls.2014.00096>.
- Takahashi, M., Feng, Z., Mikhailova, T.A., Kalugina, O.V., Shergina, O.V., Afanasieva, L.V., Heng, R.K.J., Majid, N.M.A., Sase, H., 2020. Air pollution monitoring and tree and forest decline in East Asia: a review. *Sci. Total Environ.* 140288. <https://doi.org/10.1016/j.scitotenv.2020.140288>.
- Thole, J.M., Nielsen, E., 2008. Phosphoinositides in plants: novel functions in membrane trafficking. *Curr. Opin. Plant Biol.* 11, 620–631. <https://doi.org/10.1016/j.pbi.2008.10.010>.
- Tsaluchidou, S., Cocchi, M., Tonello, L., Puri, B.K., 2008. Fatty acids and oxidative stress in psychiatric disorders. *BMC Psychiatry* 8 (Suppl. 1), S5. <https://doi.org/10.1186/1471-244X-8-S1-S5>.
- Tuominen, A., 2013. Defensive strategies in *Geranium sylvaticum*, part 2: roles of water-soluble tannins, flavonoids and phenolic acids against natural enemies. *Phytochemistry* 95, 408–420. <https://doi.org/10.1016/j.phytochem.2013.07.029>.
- Vaultier, M.N., Jolivet, Y., 2015. Ozone sensing and early signaling in plants: an outline from the cloud. *Environ. Exp. Bot.* 114, 144–152. <https://doi.org/10.1016/j.envexpbot.2014.11.012>.
- Viegas, M.C., Bassoli, D.G., 2007. Utilização do índice de retenção linear para caracterização de compostos voláteis em café solúvel utilizando GC-MS e coluna HP-Innowax. *Quím. Nova.* 30, 2031–2034. <https://doi.org/10.1590/S0100-40422007000800040>.
- Wang, A.G., Luo, G.H., 1990. Quantitative relation between the reaction of hydroxylamine and superoxide anion radicals in plants. *Plant Physiol. Commun.* 6, 55–57.
- War, A.R., Paulraj, M.G., Ahmad, T., Buhroo, A.A., Hussain, B., Ignacimuthu, S., Sharma, H.C., 2012. Mechanisms of plant defense against insect herbivores. *Plant Signal. Behav.* 7 (10), 1306–1320. <https://doi.org/10.4161/psb.21663>.
- Wittig, V.E., Ainsworth, E.A., Naidu, S.L., Karnosky, D.F., Long, S.P., 2009. Quantifying the impact of current and future tropospheric ozone on tree biomass, growth, physiology and biochemistry: a quantitative meta-analysis. *Glob. Chang. Biol.* 15, 396–424. <https://doi.org/10.1111/j.1365-2486.2008.01774.x>.
- Yadav, D.S., Rai, R., Mishra, A.K., Chaudhary, N., Mukherjee, A., Agrawal, S.B., Agrawal, M., 2019. ROS production and its detoxification in early and late sown cultivars of wheat under future O<sub>3</sub> concentration. *Sci. Total Environ.* 659, 200–210. <https://doi.org/10.1016/j.scitotenv.2018.12.352>.
- Yu, L., Fan, J., Xu, C., 2019. Peroxisomal fatty acid  $\beta$ -oxidation negatively impacts plant survival under salt stress. *Plant Signal. Behav.*, 1–3 <https://doi.org/10.1080/15592324.2018.1561121>.